AMERICAN SOCIETY FOR MICROBIOLOGY | Applied and Environmental Microbiology®

BIOTECHNOLOGY

Lipid Composition Analysis Reveals Mechanisms of Ethanol Tolerance in the Model Yeast *Saccharomyces cerevisiae*

M. Lairón-Peris,[a] S. J. Routledge,[b] J. A. Linney,[b] J. Alonso-del-Real,[a] C. M. Spickett,[b] A. R. Pitt,[b,c] J. M. Guillamón,[a] E. Barrio,[a,d] A. D. Goddard,[b] A. Querol[a]

[a]Food Biotechnology Department, Institute of Agrochemistry and Food Technology, CSIC, Valencia, Spain
[b]College of Health and Life Sciences, Aston University, Birmingham, United Kingdom
[c]Manchester Institute of Biotechnology and Department of Chemistry, University of Manchester, Manchester, United Kingdom
[d]Genetics Department, University of Valencia, Valencia, Spain

M. Lairón-Peris and S. J. Routledge contributed equally to this article. Author order was determined on the basis of alphabetical order. A. D. Goddard and A. Querol contributed equally to this article.

ABSTRACT *Saccharomyces cerevisiae* is an important unicellular yeast species within the biotechnological and the food and beverage industries. A significant application of this species is the production of ethanol, where concentrations are limited by cellular toxicity, often at the level of the cell membrane. Here, we characterize 61 *S. cerevisiae* strains for ethanol tolerance and further analyze five representatives with various ethanol tolerances. The most tolerant strain, AJ4, was dominant in coculture at 0 and 10% ethanol. Unexpectedly, although it does not have the highest noninhibitory concentration or MIC, MY29 was the dominant strain in coculture at 6% ethanol, which may be linked to differences in its basal lipidome. Although relatively few lipidomic differences were observed between strains, a significantly higher phosphatidylethanolamine concentration was observed in the least tolerant strain, MY26, at 0 and 6% ethanol compared to the other strains that became more similar at 10%, indicating potential involvement of this lipid with ethanol sensitivity. Our findings reveal that AJ4 is best able to adapt its membrane to become more fluid in the presence of ethanol and that lipid extracts from AJ4 also form the most permeable membranes. Furthermore, MY26 is least able to modulate fluidity in response to ethanol, and membranes formed from extracted lipids are least leaky at physiological ethanol concentrations. Overall, these results reveal a potential mechanism of ethanol tolerance and suggest a limited set of membrane compositions that diverse yeast species use to achieve this.

IMPORTANCE Many microbial processes are not implemented at the industrial level because the product yield is poorer and more expensive than can be achieved by chemical synthesis. It is well established that microbes show stress responses during bioprocessing, and one reason for poor product output from cell factories is production conditions that are ultimately toxic to the cells. During fermentative processes, yeast cells encounter culture media with a high sugar content, which is later transformed into high ethanol concentrations. Thus, ethanol toxicity is one of the major stresses in traditional and more recent biotechnological processes. We have performed a multilayer phenotypic and lipidomic characterization of a large number of industrial and environmental strains of *Saccharomyces* to identify key resistant and nonresistant isolates for future applications.

KEYWORDS membrane properties, *Saccharomyces cerevisiae*, ethanol

Saccharomyces cerevisiae is a unicellular eukaryotic microorganism that has been employed as a model organism to study diverse relevant phenomena in biology at

Citation Lairón-Peris M, Routledge SJ, Linney JA, Alonso-del-Real J, Spickett CM, Pitt AR, Guillamón JM, Barrio E, Goddard AD, Querol A. 2021. Lipid composition analysis reveals mechanisms of ethanol tolerance in the model yeast *Saccharomyces cerevisiae*. Appl Environ Microbiol 87:e00440-21. https://doi.org/10.1128/AEM.00440-21.

Editor Irina S. Druzhinina, Nanjing Agricultural University

Address correspondence to A. D. Goddard, a.goddard@aston.ac.uk, or A. Querol, aquerol@iata.csic.es.

Received 5 March 2021
Accepted 23 March 2021
Accepted manuscript posted online 26 March 2021
Published 26 May 2021

molecular level (1). Due to its high fermentative capability, it is also widely used in the biotechnology field for the performance of industrial fermentations of products such as wine, beer, or bread (2) or of traditional Latin American beverages such as pulque, masato, chicha, tequila, or cachaça (3–7). *S. cerevisiae* also has a relevant role in bioethanol production (8). *S. cerevisiae* has been isolated from different sources and environments all over the world, including fruits, soils, cactus, insects, oak, and cork tree barks (9, 10). The physiological and genetic diversity among the *Saccharomyces* genus is high, due to their colonization of different environments; the most studied species are those associated with industrial processes of economic importance as wine production (11–17), cider (18), and beer (11). *Saccharomyces* yeasts that have been selected to carry out these fermentations in a controlled manner show particular characteristics, as selective pressures imposed by the fermentative environment, such as low pH and the high ethanol levels in the media, favor yeasts with the most efficient fermentative catabolism, particularly *S. cerevisiae* strains, but there are species in the *Saccharomyces* genus that are also found spontaneously in these fermentation products, including *S. uvarum*. Depending on the fermentation process, other factors apart from alcohol concentration, such as temperature, can be considered stress factors (19–21).

Ethanol (CH_3CH_2OH) is a small molecule containing a methyl group and a hydroxyl group, and it is thus soluble in both aqueous and lipidic phases. Because of these properties, it can penetrate inside cells, which generates important stresses; incorporation into the cell membrane can increase fluidity, which is a fundamental driver of membrane properties (22, 23).

This fluidity change induces a loss of membrane integrity, becoming more permeable (24). Ethanol causes other detrimental effects to the cells, including alterations of mitochondrial structure, reducing ATP levels and respiratory frequency and favoring acetaldehyde and reactive oxygen species (ROS) generation, which can cause lipid peroxidation, DNA damage, and oxidative stress (25, 26). As a consequence, a notable reduction in cellular viability occurs. Cell membranes are composed of lipids (mainly phospholipids and sterols, but also sphingolipids and glycolipids) and proteins. Membrane lipids are amphipathic, possessing hydrophobic (apolar) and hydrophilic (polar) regions. Embedded membrane proteins are strongly associated with the apolar core of the bilayer and peripheral proteins are more loosely associated with the membrane via several mechanisms. A key factor contributing to membrane fluidity is the fatty acid and sterol composition of the membrane (27).

The molecular structure of ethanol allows passive diffusion across the membrane and likely incorporation into the bilayer structure (28). When this happens, van der Waals attractive forces decrease, increasing membrane fluidity (29). As determined from fluorescence anisotropy studies, a direct relationship between plasma membrane fluidity and ethanol concentration has been reported (30, 31). This increase in fluidity, together with the loss of structural integrity previously mentioned, results in loss of various intracellular components, including amino acids and ions (24), producing alterations in a cellular homeostasis.

The alterations in membrane properties are fundamental in the mechanism of ethanol toxicity, but the physical changes that the membrane structure undergoes as a result of ethanol presence in the media have not been completely described. It is widely accepted that ethanol is intercalated in lipidic heads of the membrane, with the OH group of the ethanol associated with the phosphate group of the lipidic heads and the hydrophobic tails aligned with the hydrophobic core of the membrane. When this interaction takes place, ethanol molecules substitute interfacial water molecules, generating lateral spaces between polar heads and, as a consequence, spaces in the hydrophobic core (32). These gaps result in unfavorable energy, so the system tries to minimize it by creating an interdigitated phase. This modification in the membrane causes a decrease in its thickness of at least 25% (33, 34); as a consequence of this thinning, alterations in membrane protein structure and function can occur, leading to cellular inactivation during the fermentation process (35).

It has been demonstrated that membrane thickness affects membrane protein functionality, in which maximum activity takes place with a defined thickness (36, 37). If this thickness changes, exposure of hydrophobic amino acid residues in integral membrane proteins can take place, resulting in a phenomenon known as hydrophobic maladjustment (35) that can lead to aggregation of membrane proteins to minimize the exposition of their hydrophobic parts in the aqueous media (38). Studies that use membrane models formed by phosphatidylcholine and ergosterol that are exposed to different ethanol concentrations have demonstrated that the lipid composition protects the membrane because interdigitated phase formation is delayed (39).

In Arroyo-López et al. (40) different S*accharomyces* species were characterized for their ethanol tolerance, identifying *S. cerevisiae* as the most ethanol tolerant. Here, we have selected 61 *S. cerevisiae* strains from different origins and isolation sources. The purpose of this study was to establish differences in the behavior of strains that represent the different *S. cerevisiae* groups in order to determine the most resistant ones so that they are better to perform industrial fermentations. With this aim, we both monitored the growth in a liquid medium with different ethanol concentrations, using absorbance measurements, and in a solid media, carrying out drop test analyses on ethanol plates. Growth data were statistically analyzed for each of the *S. cerevisiae* strains, and strains showing a different behavior under ethanol stress were selected to conduct membrane studies that allow correlations of lipid composition in yeast populations with responses to environmental stress such as ethanol.

RESULTS

Ethanol tolerance of the strains in solid media. A total of 61 yeast strains belonging to *S. cerevisiae* were selected to assess ethanol tolerance. The strains were identified by sequencing of the D1/D2 26S; sequencing of the D1/D2 26S rRNA gene was deposited in GenBank under accession numbers MW559910 to MW559970. All of the strains have been identified as *S. cerevisiae*, with the exception of MY62, which is an *S. cerevisiae* strain containing a limited amount of *S. kudriavzevii* genome. A total of 21 are industrial strains and were selected for their use in winemaking, and 40 of them belong to the IATA-CSIC collection. The sources from which these 40 strains were retrieved are diverse: agave, beer, bioethanol, chicha, cider, cocoa, honey water, masato, sake, sugar cane, wine, natural wild strains, etc. *S. cerevisiae* yeast strains' ethanol tolerance was first assessed in plates with GPY (glucose, peptone, and yeast extract) plus different ethanol percentages. To observe the influence of ethanol on these strains, we performed four biological replicates of each strain growth in six different media. One biological replicate for each of the strains and media can be seen in Fig. S1 in the supplemental material. With the growth data of each of the strains and taking into account the four replicate values of growth for each strain, a heatmap with the growth data in ethanol was constructed (Fig. 1). This heatmap is hierarchically clustered into two big clusters with different subclusters. The first cluster is made up of the strains that are more tolerant of ethanol (a total number of 22 of the 61 strains), and another one is made up with the rest of the strains which show intermediate and low growth with this compound (39 strains). Among the first cluster, with the most tolerant strains, it is interesting that 19 of the 22 strains belong to commercial wine strains. The other three strains included in this heatmap are AJ4, a Lallemand commercial strain that is also one of the most tolerant strains of all the screened strains; MY48, a cachaça strain; and MY43, a cider yeast strain.

The other cluster, with the 39 intermediate- to low-tolerance strains, appears to be divided into two subclusters, too. One of the subclusters is composed of MY33 and MY34, which are less ethanol tolerant and belong to the sake group. It is interesting to note that in the other subcluster there are strains with different behaviors. For example, the growth of strains MY46 (cachaça) and MY44 (cider) in ethanol media is affected by low ethanol concentrations (6% ethanol), but they can grow (at a low rate) until 16% of ethanol is present in solid media. On the other hand, there are other strains,

FIG 1 Heatmap representation of growth values (from 0 to 3) of the analyzed strains at plates with increasing ethanol concentrations. Each line corresponds to a strain (AJ4, MY1 to MY63), and each column corresponds to a particular ethanol

(Continued on next page)

such as MY37 (Masato) and MY22 (natural), whose growth is not affected until 10% ethanol is present in GPY solid media, but at the next ethanol step (14%) they do not grow at all.

Ethanol tolerance of the strains in liquid media. The ethanol tolerance of the set of *S. cerevisiae* strains was evaluated in minimal YNB (Difco) liquid medium at 28°C. Yeast growth was evaluated by determining the optical density at 600 nm (OD_{600}) in microtiter plates containing this medium with different ethanol concentrations and, for each strain, the area under the curve during these growths was calculated. With the area under the curve reduction due to the addition of ethanol, the NIC (noninhibitory concentration) and MIC parameters were calculated for 57 of the 61 strains. Not all of the 61 strains could be evaluated using this method: the data obtained with flor yeast strains MY28 and MY31 could not be used because these strains flocculate, and the data obtained with them are not reproducible. The data obtained with strains MY55 and MY56 were not used since these strains have problems growing in the minimal medium YNB. The complete list with the NIC and MIC values for each one of the selected strains can be found in Table S1 in the supplemental material. Figure 2 depicts a graph representing these values for each one of the strains.

Strain selection. We phenotypically characterized our collection of 61 strains in ethanol. To further characterize some representatives of the different behaviors, we decided to select five of them since they showed a range of tolerances: AJ4, MY3, MY14, MY26, and MY29. Figure 3A shows the results of the drop test in GPY-ethanol (GPY plus ethanol) medium of these five strains, and Fig. 3B shows the NIC and MIC parameters of growth in YNB liquid medium-ethanol.

AJ4 shows high NIC and MIC values during YNB growth in liquid media, and in solid medium in GPY-ethanol it clusters among the most tolerant *S. cerevisiae* strains, too. This strain is a Lallemand commercial strain that has been reported as a highly tolerant ethanol strain (41). It has a high NIC value of 11.62% $\pm$ 0.33%, which means that a high concentration of ethanol is needed to affect its growth.

MY29, a flor strain isolated from sherry wine, is classified within the second cluster with the strains that show an intermediate growth in GPY-ethanol in solid media. It grows well until 14% ethanol; however, viability is reduced in 16% ethanol, and it is unable to grow in 18% ethanol. Regarding the liquid assay in YNB-ethanol, the MIC value is among the highest MIC values of all the strains (15.41% $\pm$ 2.93%), but its NIC value (7.5% $\pm$ 1.48%) can be classified as a medium to low. This result shows that MY29 is an *S. cerevisiae* strain whose behavior can be classified as intermediate under ethanol conditions. Moreover, MY29 is the most tolerant sherry wine strain of the five strains analyzed.

MY26, an agave strain, is among the least tolerant strains in solid media and is also the strain that shows the lowest growth among the three agave strains that we selected for our study. In liquid media, its NIC value is also low, since it is affected by an ethanol concentration of 7.24% $\pm$ 0.77%, but its MIC value is high (15.34% $\pm$ 0.4%). This strain shows a behavior in liquid media similar to that of MY29, but in solid media it proved to be less tolerant since it was not able to grow in 14% ethanol plates, and MY26 could grow in this condition, as well.

MY3 and MY14 are commercial wine strains, which are classified in the cluster of the most tolerant strains regarding their growth on ethanol plates. Nevertheless, MY14 appears to be affected by the ethanol at low concentrations (NIC value of 6.787% $\pm$ 0.337% and MIC value of 13.93% $\pm$ 0.91%), and MY3 seems to start being affected by ethanol at higher concentrations but has a low range, since it has a low MIC value (NIC 8.89% $\pm$ 1.26% and MIC 12.97% $\pm$ 0.13%).

FIG 1 Legend (Continued)
concentration (0, 6, 10, 14, 16, and 18%). The color key bar at the top indicates growth values, from yellow (low growth value) to pink (high growth value). Hierarchical clustering is showed on the left. Color dots on the right of the figure indicate the source or origin of each one of the strains, and shapes indicate their classification. See Fig. S1 to view one of the four replicates from which these heatmaps were constructed.

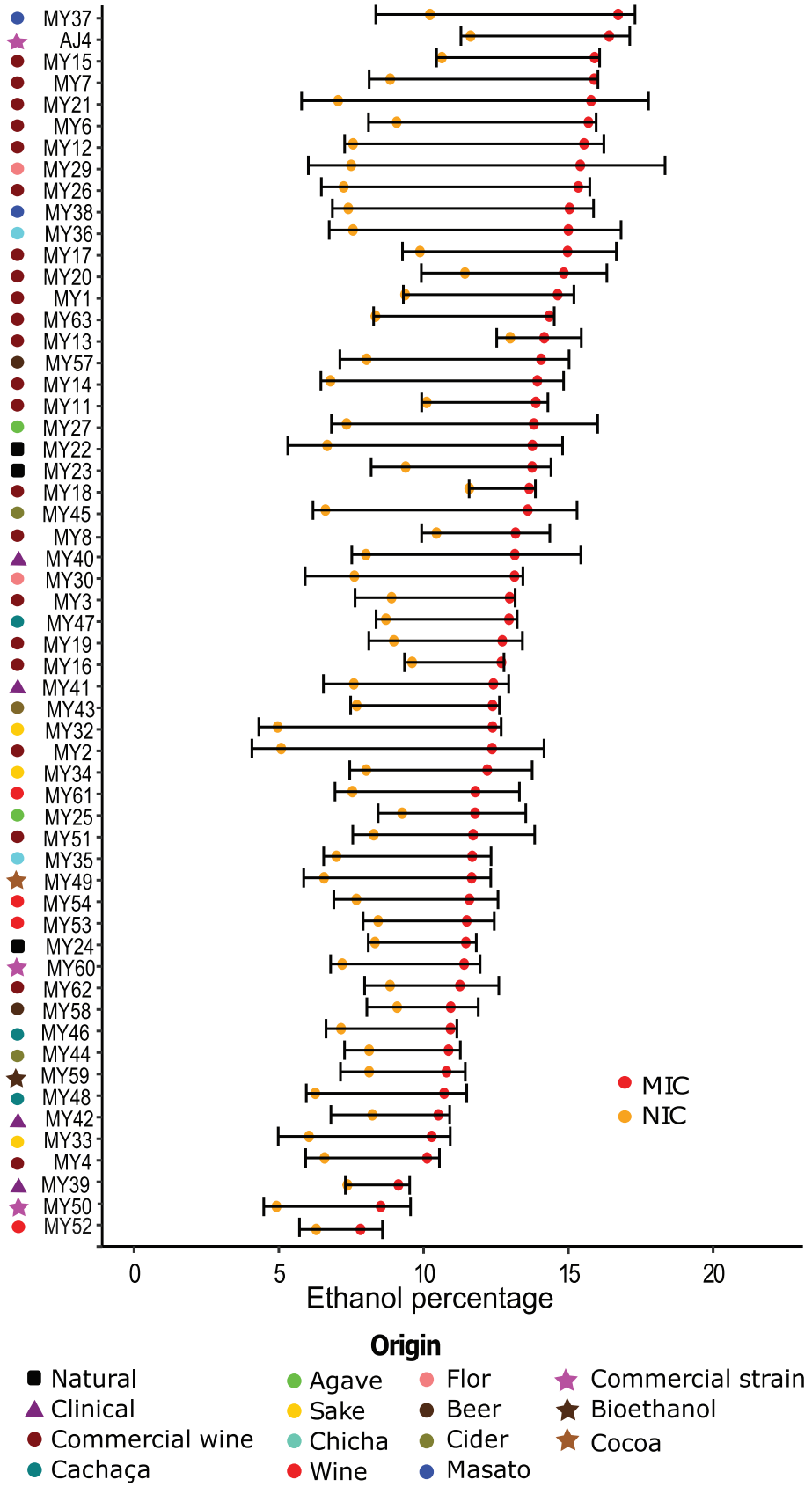

FIG 2 Representations of NIC (yellow) and MIC (red) parameters for the selected strains in relation to its ethanol tolerance (%). Values are averages from triplicate experiments, and standard deviations are represented also. Color dots on the right of the figure indicate the source or origin of each one of the strains, and shapes indicate their classification. Strains are ordered by MIC value.

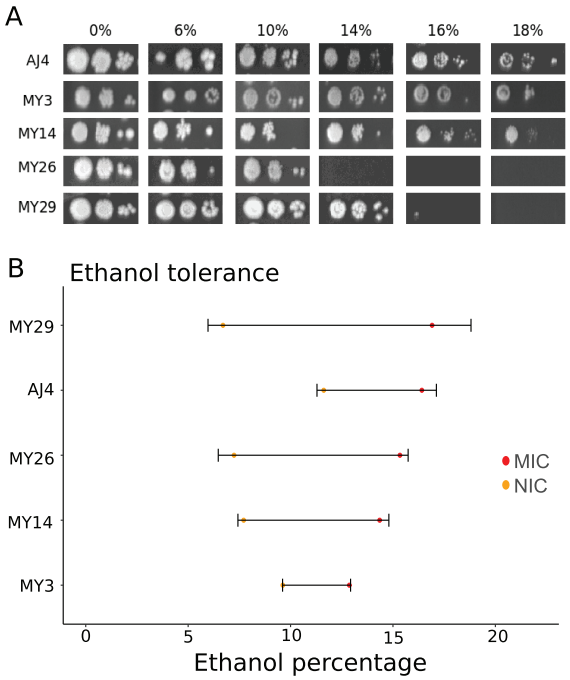

FIG 3 (A) Photographs of the drop tests in ethanol plates. (B) NIC and MIC parameters for each of five selected strains.

Competition fermentations. These five strains—AJ4, MY3, MY14, MY26, and MY29—were selected for their different behaviors regarding ethanol susceptibility. They were inoculated into mixed culture fermentations to assess the correlation between ethanol tolerance and competition capacity under different ethanol concentrations (0, 6, and 10%). Since one GPY fermentation would be insufficient for observing domination of the culture by a single strain, we inoculated a sample of the culture after sugar depletion into new fresh media with the corresponding ethanol concentration.

After the tenth pass, AJ4 completely dominated the 0 and 10% fermentations. However, in 6% fermentations, the MY29 strain completely dominated one of the three replicate fermentations and clearly dominated the other two. The other two strains present in this 6% fermentation when sugar is depleted are AJ4 and MY14, although in low proportions. Neither MY3 nor MY26 colonies were found in any of the fermentation (Fig. 4). AJ4 dominating high ethanol concentration cultures was an expected result considering its ethanol tolerance determined in the present study. However, it does not seem clear why MY29 dominates 6% ethanol cultures, given its moderate tolerance compared to other strains such as AJ4, MY3, or even MY14. Here, probably, complex interaction among strains plays an important role in domination, which has

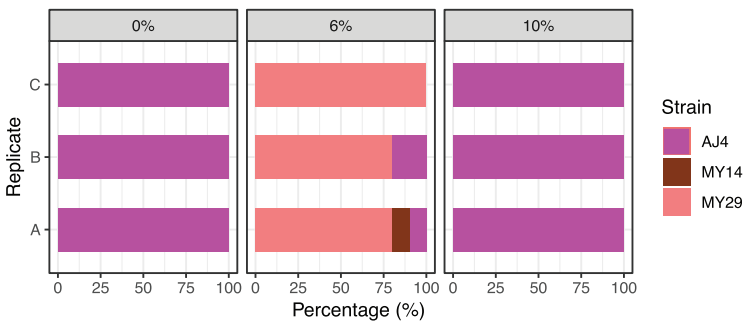

FIG 4 Percentages of strains present in GPY-ethanol medium determined by molecular identification after 10 rounds of fermentations. Every biological replicate is indicated by the letters A, B, and C, and the ethanol concentration present in the media is shown on the *x*-axis.

been studied previously for another set of strains (42) and demonstrated to be important together with growth capacity under the studied medium conditions (43).

Lipid composition and membrane properties. Several studies have demonstrated that yeasts can adapt their membrane composition in response to ethanol stress (44–46). To better understand the effects of ethanol upon the yeast strains, we investigated the properties of the membranes in the presence or absence of ethanol. We determined the total lipid compositions of each strain by mass spectrometry (see Tables S2 and S3 in the supplemental material). The numbers of species identified for major lipid classes for strains grown in media containing 0 or 6% ethanol are shown in Fig. 5. For strains grown in the absence of ethanol, among the ceramide 1-phosphates (CerP) there were significantly fewer species observed in MY29 (109.6 ± 6.61) than in AJ4 and MY3 (128.2 ± 1.49 and 130 ± 0.55), where $P < 0.01$ (two-way analysis of variance [ANOVA] and Tukey's multiple-comparison test) and MY14 (126.6 ± 1.86), where $P < 0.05$. For cardiolipin species (CL), there were significantly fewer observed in AJ4 and MY3 (3.0 ± 0.45 and 3.0 ± 0.31; $P < 0.01$) and MY14 and MY26 (4.2 ± 1.3 and 4.0 ± 0.55; $P < 0.05$) compared to MY29 (9.67 ± 1.8). There were fewer diacylglycerols observed in MY29 compared to MY3 (180.2 ± 1.93 and 193.0 ± 1.41; $P < 0.05$). For glycerophosphatidic acid (GPA) species, there were significantly fewer species identified for MY29 (126.4 ± 15.17) than for AJ4 (178.0 ± 2.28; $P < 0.0001$), MY3 (175.0 ± 1.05; $P < 0.001$), MY14 (170.4 ± 5.30; $P < 0.001$), and MY26 (167.8 ± 6.67; $P < 0.01$). There were also fewer glycerophosphatidylethanolamine (GPEth) species identified for MY29 compared to each of the strains ($P < 0.01$ in each case): 259.6 ± 3.2 for AJ4, 258.4 ± 1.36 for MY3, 254.8 ± 2.85 for MY14, 252.4 ± 3.26 for MY26, and 186.2 ± 35.034 for MY29. For glycerophosphoserine species (GPSer), there were fewer species in MY29 (120.0 ± 12.99) compared to AJ4 and MY3 (157.6 ± 2.50 and 159 ± 1.41; $P < 0.001$), MY14 (151.6 ± 3.41; $P < 0.01$), and MY26 (147.4 ± 3.94; $P < 0.05$). Lastly, there were fewer monoacylglycerol (MG) species observed in MY29 (19.0 ± 0.84) than in MY3 (24.6 ± 0.51; $P < 0.01$).

There were no significant differences observed between the species grown in the presence of 6% ethanol; however, significant changes were seen between the 0 and

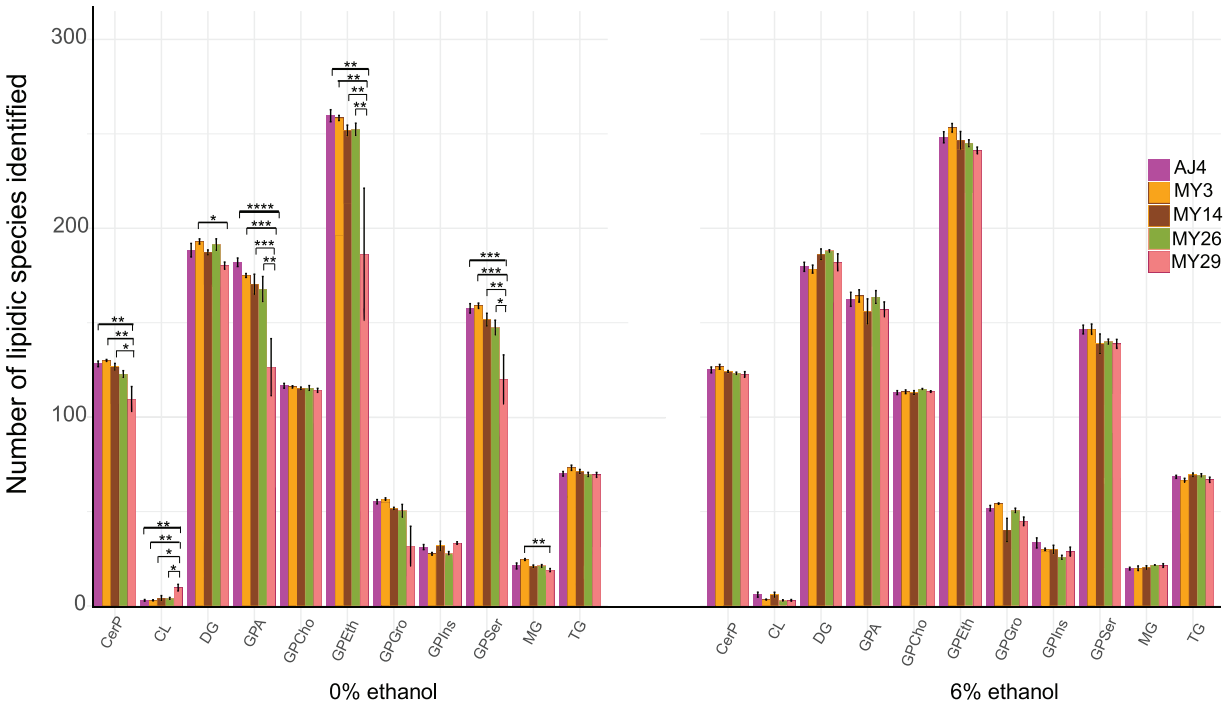

FIG 5 Number of species identified by lipid class for AJ4, MY3, MY14, MY26, and MY29 strains in the presence of 0% and 6% ethanol. Lipids were extracted and analyzed by LC-MS in positive- and negative-ion modes ($n = 5$).

6% ethanol samples. For CL, there were significantly fewer species observed for MY29 grown at 6% ethanol than at 0% ethanol (3.0 ± 0.44 and 9.66 ± 1.80; $P < 0.01$). For DG, there were more species in MY3 grown at 0% ethanol than at 6% ethanol (193.0 ± 1.41 and 178.4 ± 2.13; $P < 0.05$). For GPA, there were significantly fewer species in MY29 grown at 0% ethanol than at 6% ethanol (126.4 ± 15.17 and 157.0 ± 4.03; $P < 0.05$), and for GPEth, there were also significantly fewer species in MY29 grown at 0% than at 6% ethanol (186.2 ± 35.04 and 241.2 ± 1.82; $P < 0.05$). There were significantly more MG species in MY3 grown at 0% ethanol (24.6 ± 0.51 and 20 ± 1.22; $P < 0.05$) and more TG species in MY3 grown at 0% ethanol than at 6% ethanol (73.2 ± 1.39 and 66.6 ± 1.03; $P < 0.01$). Strikingly, MY29 seems to have the most different total lipid composition at 0% ethanol and to remodel this most dramatically, in terms of species diversity, at 6%. However, at 6% ethanol, the species diversity in MY29 was similar to the other strains, perhaps indicating an optimal membrane composition for ethanol tolerance.

Acyl chain length and saturation have been shown to be important factors in regulating membrane fluidity and ethanol tolerance in yeast (44–46). We therefore investigated this for AJ4, MY3, MY14, MY26, and MY29 strains in both 0 and 6% ethanol. Although there were no significant changes in average carbon length of the acyl chains for each of the strains grown in 0% compared to 6% ethanol (see Fig. S2), there were significant differences in saturation (Fig. 6). For the strains grown in 0% ethanol

FIG 6 Percentages of saturated, monounsaturated, and polyunsaturated chains by lipid class showing significant changes for AJ4, MY3, MY14, MY26, and MY29 strains in the presence of 0% ethanol (A) and for AJ4, MY3, MY14, MY26, and MY29 strains in the presence of 6% ethanol (B). Lipids were extracted and analyzed by LC-MS in positive- and negative-ion modes ($n = 5$).

(Fig. 6A), DG species contained a significantly lower percentage saturated acyl chains in MY29 compared to AJ4 (37.95 ± 0.35 and 40.22 ± 0.30; $P < 0.01$). There was a significantly higher percentage of monounsaturated CL species in MY29 (30 ± 7.83) compared to AJ4 and MY3 (0 ± 0.0 in both cases; $P < 0.01$) and MY26 (3.33 ± 3.33; $P < 0.05$). For GPA, there was a significantly higher percentage saturated chains in MY29 (34.51 ± 1.07) compared to MY14 (31.30 ± 0.88; $P < 0.05$). For GPEth, there were more saturated chains in MY29 compared to AJ4, MY3, MY14, and MY26 (31.21 ± 3.79, 25.30 ± 0.24, 24.92 ± 0.16, 24.96 ± 0.26, and 24.38 ± 0.26; $P < 0.05$ in each case). There was a significantly greater number of saturated GPSer species in MY29 compared to MY26 (32.44 ± 1.70 and 29.24 ± 0.22; $P < 0.05$) and a lower number of monounsaturated species in MY29 (40.07 ± 2.20) compared to MY3 and MY14 (45.11 ± 0.62 and 44.7 ± 0.59; $P < 0.05$). Lastly, there was a significantly higher percentage of MG species containing two unsaturations in MY29 (10.59 ± 0.40) compared to MY3 (8.14 ± 0.17; $P < 0.05$). Once again, MY29 was the most different in terms of saturated species at 0% ethanol and remodels its membrane to be more similar to the other strains at 6%.

There were no significant differences observed between strains for 6% ethanol samples (Fig. 6B), but there were significant differences between strains grown in 0% compared to 6% ethanol. There was a significantly higher percentage of saturated DG species for AJ4 at 0% than at 6% ethanol (40.22 ± 0.30 and 38.08 ± 0.44) and a lower percentage of monounsaturated species for AJ4 (32.80 ± 0.09 and 34.75 ± 0.38; $P < 0.001$) and MY3 (33.06 ± 0.21 and 34.54 ± 0.25; $P < 0.05$) at 0% compared to 6% ethanol. For saturated GPEth species, there was a significantly higher percentage in MY29 at 0% ethanol than MY29 at 6% ethanol (31.21 ± 3.79 and 24.65 ± 0.26; $P < 0.05$) and significantly fewer monounsaturated species in MY29 at 0% ethanol compared to MY29 at 6% ethanol (40.23 ± 0.55 and 41.94 ± 0.42; $P < 0.05$). There were significantly more monounsaturated glycerophosphoglycerol (GPGro) species in MY29 at 0% ethanol compared to 6% ethanol (19.12 ± 4.95 and 12.37 ± 1.05). In addition, there were significantly fewer monounsaturated GPSer species in MY29 at 0% ethanol than in MY29 at 6% ethanol (40.07 ± 2.20 and 44.77 ± 0.23). Lastly, for TG species, there were significantly more saturated species in MY14 at 0% ethanol than in MY14 at 6% ethanol (35.94 ± 0.58 and 30.86 ± 1.16; $P < 0.001$), more monounsaturated species in AJ4 at 6% ethanol (26.33 ± 0.503; $P < 0.01$), MY14 at 6% ethanol (6.24 ± 0.55; $P < 0.01$), and MY26 at 6% ethanol (25.73 ± 0.26; $P < 0.05$) compared to the 0% samples (23.40 ± 0.64, 23.60 ± 0.40, and 23.55 ± 0.25, respectively), and fewer species containing two unsaturations in MY3 (26.50 ± 0.47; $P < 0.01$) and MY14 at 0% (26.98 ± 0.55; $P < 0.05$) compared to the 6% (29.43 ± 0.68 and 29.39 ± 0.48) samples.

To assess variation in overall lipid unsaturation, the unsaturation index (UI) was calculated at the lipid level by lipid class for species identified in each strain at 0 and 6% ethanol (Table 1) using the percentage of lipids weighted by the number of unsaturated bonds: UI = % with one unsaturation + (2 × % with two unsaturations) + (3 × % with three unsaturations) + (4 × % with four unsaturations). The UI for DG was significantly lower for AJ4 compared to MY29 at 0% ethanol (86.76 ± 0.64 and 90.03 ± 0.61, $P < 0.01$) and higher for GPEth species in the 0% ethanol AJ4, MY14, and MY26 strains compared to MY29 (108.72 ± 0.35, 108.72 ± 0.28, 109.36 ± 0.60, and 97.36 ± 7.13, respectively; $P < 0.05$ in each case). The UI for MY29 at 0% ethanol was also significantly lower than at 6% ethanol (108.73 ± 0.92, $P < 0.05$). Lastly, the UI for MG species at 0% ethanol was significantly lower for MY3 compared to MY29 (73.30 ± 16.58 and 83.27 ± 18.95; $P < 0.05$), and the UI for MY29 at 0% ethanol was significantly higher compared to MY29 at 6% ethanol (83.27 ± 18.95 and 78.74 ± 1.52; $P < 0.05$).

Due to changes observed in phosphatidylethanolamine (PE) and phosphatidylserine (PS) species diversity in Fig. 5, we undertook quantitative thin-layer chromatography (TLC) analysis of these lipids. This showed significant differences in the abundance of PE in MY26 grown in 0% ethanol (0.41 ± 0.02), where the abundance was higher compared to AJ4 (0.03 ± 0.01; $P < 0.0001$), MY3 (0.08 ± 0.01; $P < 0.0001$), MY14 (0.17 ± 0.01; $P < 0.0001$), and MY29 (0.18 ± 0.04; $P < 0.0001$) grown in 0% ethanol, as

TABLE 1 Unsaturation index for lipids identified in each strain

Lipid species	UI ± SD[a]									
	0% ethanol					6% ethanol				
	AJ4	MY3	MY14	MY26	MY29	AJ4	MY3	MY14	MY26	MY29
CerP	41.38 ± 1.09	42.50 ± 1.01	41.86 ± 0.54	41.90 ± 0.50	40.23 ± 4.34	83.25 ± 0.58	82.93 ± 0.41	84.39 ± 1.17	83.93 ± 0.43	83.25 ± 0.58
CL	33.33 ± 13.92	70.00 ± 8.15	62.22 ± 23.36	90.00 ± 31.83	88.00 ± 35.91	107.24 ± 34.56	60.00 ± 4.08	111.79 ± 32.31	30.00 ± 19.96	84.33 ± 32.53
DG	**86.76 ± 0.64**	89.02 ± 0.29	88.99 ± 0.62	89.25 ± 0.48	**90.03 ± 0.61**	89.10 ± 4.08	89.91 ± 0.31	88.31 ± 0.63	87.65 ± 0.64	89.71 ± 0.69
GPA	104.16 ± 0.98	103.65 ± 0.34	107.60 ± 1.63	104.22 ± 1.01	103.12 ± 0.87	103.96 ± 23.31	104.26 ± 1.00	105.53 ± 0.34	104.08 ± 1.02	105.09 ± 1.13
GPCho	50.20 ± 0.57	50.29 ± 0.17	50.03 ± 0.43	50.72 ± 0.32	50.36 ± 0.35	96.64 ± 19.96	96.66 ± 0.49	96.47 ± 0.59	96.35 ± 0.50	95.77 ± 0.71
GPEth	**108.72 ± 0.35**	108.20 ± 0.35	**108.72 ± 0.28**	**109.36 ± 0.60**	**97.36 ± 7.13**	109.69 ± 32.53	110.43 ± 0.50	110.04 ± 1.06	109.81 ± 0.36	**108.73 ± 0.92**
GPGro	124.20 ± 0.97	123.76 ± 1.02	119.56 ± 1.01	124.69 ± 2.03	125.84 ± 5.31	121.53 ± 3.14	120.00 ± 0.31	120.03 ± 2.85	120.87 ± 2.67	127.20 ± 2.24
GPIns	82.24 ± 1.21	88.80 ± 3.42	80.55 ± 2.65	88.05 ± 3.25	92.06 ± 2.02	81.06 ± 2.40	84.26 ± 1.81	85.24 ± 4.14	90.56 ± 2.16	86.07 ± 2.39
GPSer	96.68 ± 0.59	95.85 ± 0.33	95.92 ± 0.62	97.30 ± 0.43	95.06 ± 1.70	97.83 ± 22.32	96.80 ± 22.09	96.52 ± 22.01	97.00 ± 22.13	96.68 ± 22.05
MG	77.42 ± 17.68	**73.30 ± 16.58**	78.09 ± 17.71	78.43 ± 17.77	**83.27 ± 18.95**	79.90 ± 1.88	83.21 ± 1.26	80.59 ± 2.78	78.74 ± 0.90	**78.74 ± 1.52**
TG	116.88 ± 1.35	118.43 ± 2.36	118.00 1.16	114.93 ± 0.62	118.19 ± 0.54	118.75 ± 1.18	120.76 ± 1.65	125.55 ± 2.90	118.22 ± 0.91	122.29 ± 1.91

[a]The unsaturation index (UI) for lipids identified in each strain was calculated using the percentage of lipids with each number of unsaturated bonds: one unsaturation + (2 × two unsaturations) + (3 × three unsaturations) + (4 × four unsaturations). Statistically significant differences between strains and ethanol conditions are highlighted in boldface (two-way ANOVA and Tukey's multiple-comparison test [$n = 5$]).

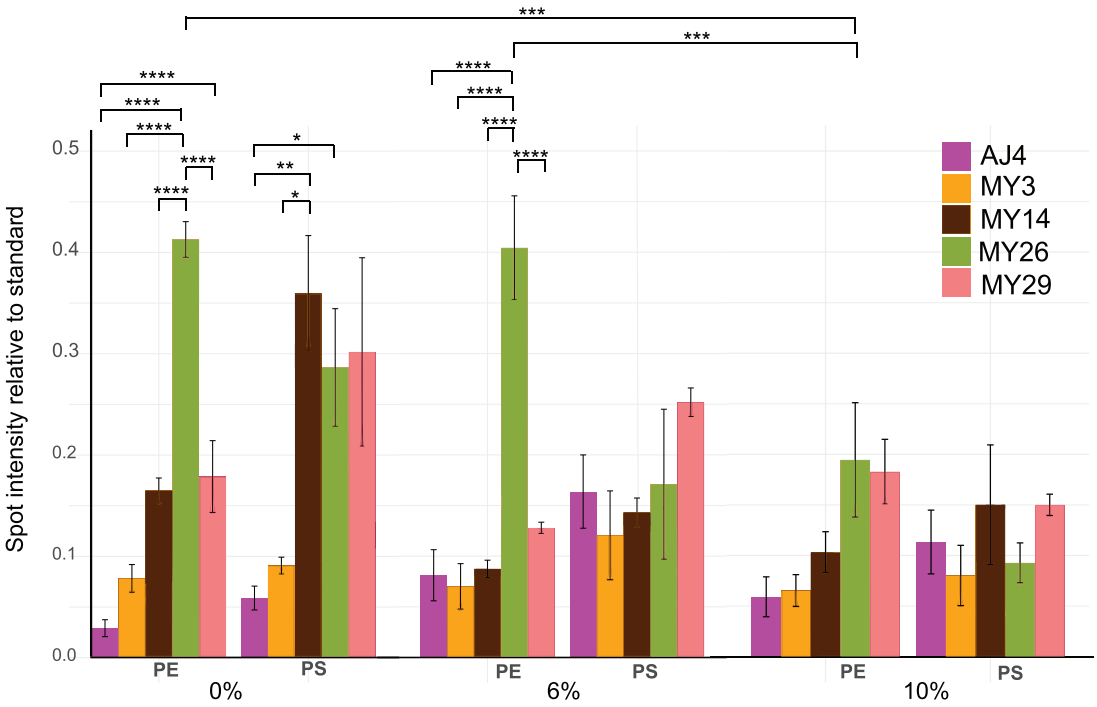

FIG 7 TLC analysis of phosphatidylethanolamine (PE) and phosphatidylserine (PS) abundance for AJ4, MY3, MY14, MY26, and MY29 strains in the presence of 0, 6, or 10% ethanol. Samples were loaded in triplicate, and the spot intensity was analyzed using ImageJ. The spot intensity is plotted relative to phospholipid standards loaded onto each plate.

illustrated in Fig. 7. At 6% ethanol, there was also a significantly greater abundance of PE in MY26 (0.41 ± 0.05) compared to AJ4 (0.08 ± 0.03; $P < 0.05$), MY3 (0.07 ± 0.02; $P < 0.0001$), MY14 (0.09 ± 0.01; $P < 0.0001$), and MY29 (0.13 ± 0.01; $P < 0.0001$). In addition, there was a lower abundance of PE in MY26 at 10% ethanol (0.20 ± 0.06) compared to MY26 at both 0% ethanol (0.41 ± 0.02) and 6% ethanol (0.41 ± 0.051; $P < 0.001$). There was a significantly lower abundance of PS in AJ4 at 0% ethanol (0.06 ± 0.01) compared to MY14 and MY29 (0.36 ± 0.06 and 0.30 ± 0.09; $P < 0.01$ and $P < 0.05$, respectively). There was also a significantly lower abundance of PS in MY3 compared to MY14 at 0% ethanol (0.09 ± 0.01 and 0.36 ± 0.06; $P < 0.05$). It is notable that MY26, the least tolerant strain, is the most different at 0 and 6% ethanol but has a composition similar to the other strains at 10%.

We next examined the effect of ethanol upon the fluidity of the yeast membranes as they grew in cultures with or without ethanol. We utilized the fluorescent dye, Laurdan, which has been used to study phase properties of membranes since it is sensitive to the polarity of the membrane environment (47). GP (generalized polarization) values, which correlate inversely with fluidity, were calculated at six time points during the growth of AJ4, MY3, MY14, MY26, and MY29 strains in GPY alone, GPY containing 6% ethanol, and GPY containing 10% ethanol. The assay suggests that the fluidity of the yeast membranes decreases with culture time, as shown by the increase in GP (Fig. 8). AJ4 and MY14 strains demonstrated large changes in fluidity when treated with 10% ethanol (AJ4 showed a GP value change of -0.0002 ± 0.0009 at 10% and a GP value change of 0.0233 ± 0.0025 at 0%, and MY14 showed a GP value change of -0.0101 ± 0.002 at 10% and a GP value change of 0.009 ± 0.002 at 0%; $P < 0.001$ and $P < 0.01$, respectively). MY29 also became significantly more fluid at 10% ethanol (GP value change of -0.0016 ± 0.0011 at 10% and a GP value change of 0.0084 ± 0.0019 at 0%; $P < 0.05$). However, these strains did not show any increases in fluidity with 6% ethanol. The other strains showed no significant differences to fluidity with ethanol treatment. It is notable that the most tolerant strains show the largest increases in membrane fluidity in response to ethanol exposure.

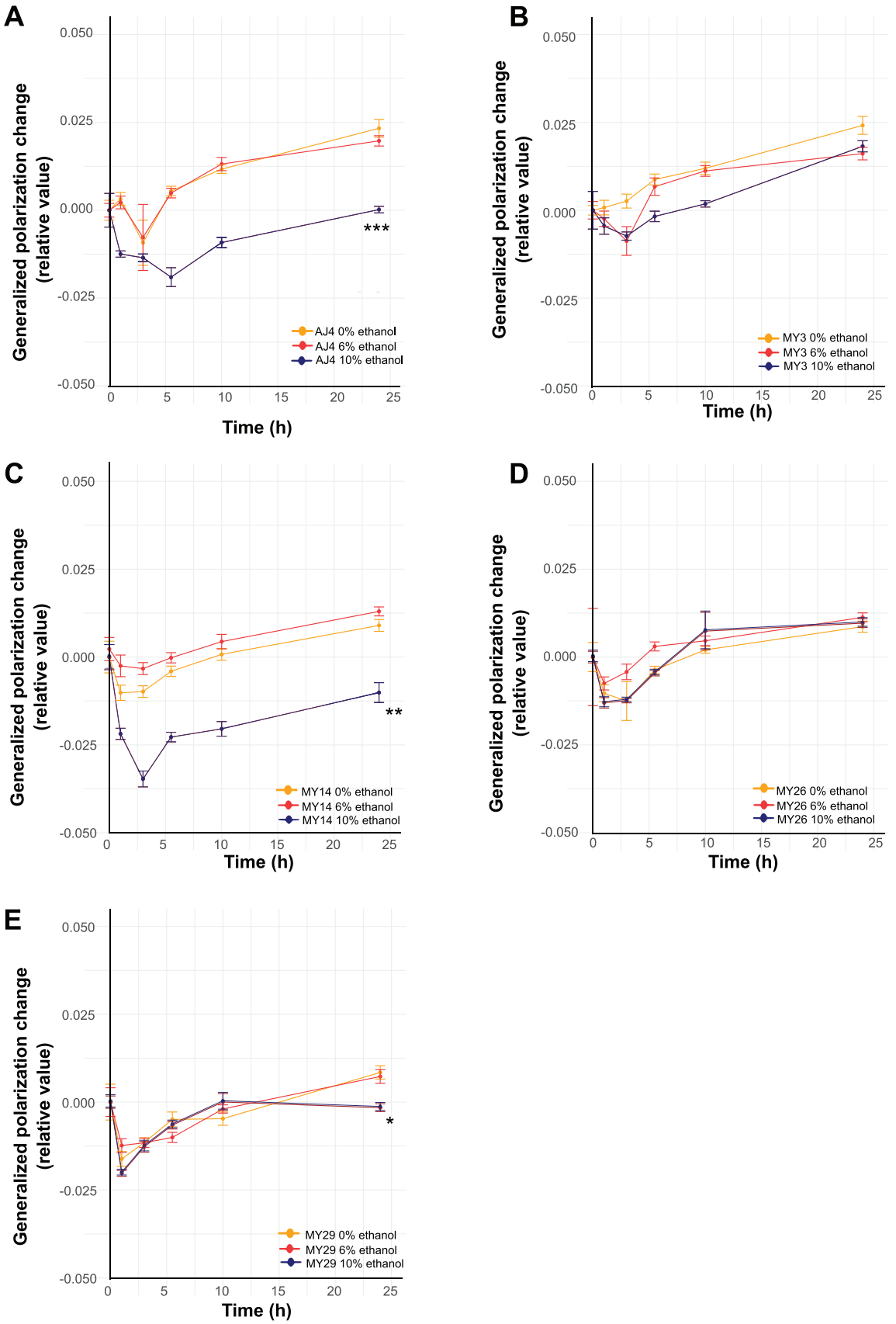

FIG 8 Effects of ethanol upon the fluidity of live yeast throughout the fermentation, measured by changes to Laurdan generalized polarization (GP).

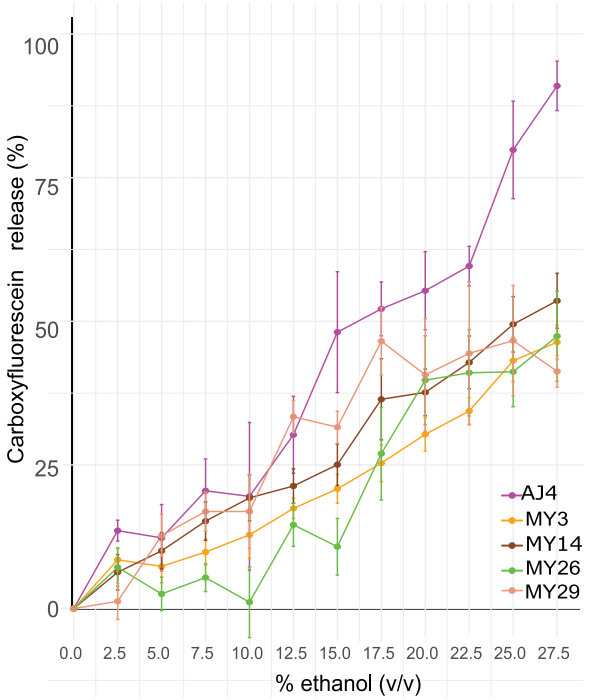

FIG 9 Effects of ethanol upon liposomes composed of lipids extracted from AJ4, MY3, MY14, MY26, and MY29 strains normalized to the maximum amount of dye released upon treatment with 5% Triton X-100.

To examine membrane permeability, we investigated the integrity of liposomes composed of lipids extracted from each of the strains and loaded with carboxyfluorescein (CF) dye. The liposomes were challenged with increasing concentrations of exogenous ethanol, and the fluorescence increase from CF dye release was measured. The data in Fig. 9 show that the liposomes containing lipids extracted from AJ4 demonstrated a significantly greater increase in fluorescence at high ethanol concentrations than those composed of lipids from the other strains (ANOVA and Tukey's multiple-comparison test (90.98 ± 4.29 fluorescence increase; $P < 0.001$). MY3 and MY26 liposomes were less "leaky" overall (46.38 ± 2.97 and 47.41 ± 7.84 of fluorescence increase). This increase in fluorescence indicates increased "leakiness" of the membranes.

Principal-component analysis. With the aim of grouping the five selected strains based on their lipid composition and their ethanol tolerance, the data obtained in the previous sections was used to perform a principal-component analysis (PCA) (Fig. 10). The data from the variables NIC, MIC, and the drop test growth value at 14 and 16% of ethanol in the plates, related to the ethanol tolerance, were used. For the lipid composition, the data of the CF release at the last time point; the data from the Laurdan experiments of the differential GP value at 10% ethanol and when no ethanol was present at the last time point and the PE abundance at 0 and 6% ethanol in the media were used. The two commercial wine strains MY3 and MY14 group together, and MY26 (the most sensitive to ethanol) and AJ4 (the most tolerant) are the two strains that demonstrate the most differences among them. It is interesting that MY26 is associated in the PCA with an accumulation of PE in the membrane at a low ethanol concentration and a higher membrane rigidity and that the most tolerant stain, AJ4, is associated with a high membrane fluidity in the presence of ethanol.

DISCUSSION

In this study, we investigated the membrane properties of the selected yeast strains to try to understand their different levels of ethanol tolerance. The mass spectrometry

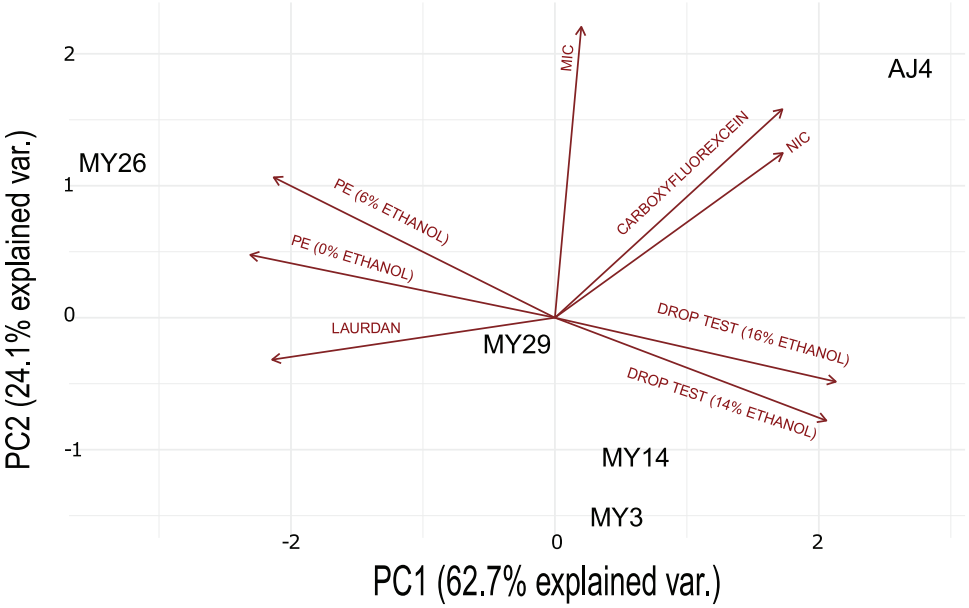

FIG 10 Plot of the first two factors of a PCA of the five *S. cerevisiae* strains versus their lipid composition and ethanol tolerance.

analysis of the lipid composition of each strain in the absence of ethanol highlighted differences, in particular between MY29 and the other strains, not only in the variety of species observed for the lipid classes but also in their saturation. MY29 is a flor yeast. These yeasts constitute a separate phylogenetic group within *S. cerevisiae* species. They are characterized by forming a layer on top of wine known as flor, which allows them to access oxygen during the fermentation of sherry wines, so they show different behaviors and thus physiological characteristics to wine yeast. Moreover, they have been reported to survive under extreme conditions (ethanol content >15%) (48, 49), which could relate to their membrane structure.

Upon treatment with 6% ethanol, the lipid composition of MY29 underwent significant changes; the composition was then found to be more similar to that of the other strains, suggesting that the membrane of MY29 underwent more drastic changes than the other strains in response to ethanol. The lack of significant differences at 6% ethanol suggests that each of the strains moves toward a more common lipid composition in response to ethanol. However, despite the fewer differences to lipid composition at 6% ethanol between the strains, MY29 dominated the fermentation at this concentration. In addition, the lipid composition of AJ4 was not significantly different from that of the other strains at 6% ethanol, although it was the most tolerant to ethanol. It is possible that there may be further adaptation of the membrane at higher ethanol concentrations than were investigated in this study, but it is likely that other factors contribute to the ethanol tolerance of these strains.

Indeed, this has been suggested by other studies, where the relationship between H^+-ATPase activity and ergosterol content, as well as the sterol/phospholipid and protein/phospholipid ratios, is important (45, 50, 51). Ethanol tolerance is a complex phenotype, and different mechanisms may lead to improved tolerance. Fluidization of the yeast membranes by ethanol is also known to activate the unfolded protein response, and it is speculated that a better response could lead to greater tolerance (52). Moreover, yeast cells can increase their tolerance to ethanol by other mechanisms, such as an increase in the biosynthesis of some amino acids, such as tryptophan (53), and trehalose accumulation (54). Nevertheless, it is striking that yeast strains with different membrane compositions in the absence of ethanol become more similar upon

exposure, suggesting a common, or limited number, of membrane compositions that maximize tolerance to ethanol.

Incorporation of longer acyl chains and a decrease in shorter chains has previously been shown to occur in yeast in response to ethanol (46, 55); however, we did not observe any significant changes in chain length. Our study does suggest that there were significant differences in saturation between the species upon ethanol treatment. These changes occurred in GPGro and GPEth in MY29, and occurred predominantly in DG and TG for the other strains, with shifts toward increased saturation for AJ4 and increased unsaturation for MY3 and MY14. These changes appear to be complex and specific to each strain. Documented changes to the membrane of yeast upon ethanol challenge are conflicting (56); while some studies have shown that increased levels of unsaturated fatty acids are linked to improved ethanol tolerance (46), changes to the UI may not necessarily be associated with improved tolerance or lead to the expected changes in membrane fluidity, and it is rather the potential of the cell to alter its composition (45, 57). The lipid membrane is a highly complex environment and multiple factors can influence membrane fluidity and permeability. Further study of these strains is required to determine whether their different compositions have similar biophysical properties.

We investigated the fluidity of the membranes, and the Laurdan assay demonstrated that the fluidity of the membranes for each strain decreased over the duration of the fermentation, which has been observed previously (58), and may be linked to nutrient depletion and changes in the growth rate of the cells. In our study, the most tolerant strain, AJ4, underwent the largest changes in fluidity, where the membranes were significantly more fluid at 10% ethanol than in the other conditions. AJ4 lipid-containing liposomes were also the "leakiest" compared to the other strains. This strain may therefore be better able to tolerate the fluidizing effects of ethanol upon the membrane or to modulate its membrane composition to lead to an increase in fluidity; this more fluid composition may allow more efficient movement of ethanol across the membrane. The membranes of one of the least tolerant strains, MY26, did not alter in fluidity in any of the conditions and liposomes comprised of MY26 lipids were less leaky when challenged with ethanol. In addition, our analysis of PE abundance shows that MY26 contained significantly more PE than the other strains in both 0 and 6% ethanol, while the most tolerant strain, AJ4, contained less PE in general than other strains. PE has a small head group and can form hydrogen bonds with adjacent PE molecules (59). It influences lipid packing and therefore membrane fluidity, where increased PE content results in less-fluid membranes (60, 61), consistent with our hypothesis. A lower PE content in relation to PC has been correlated with more tolerant strains (46, 62). These findings suggest that more tolerant strains are more fluid and permeable, whereas less tolerant strains are more rigid and less permeable. Several studies have correlated membrane fluidity and ethanol tolerance, and many of these point to increased fluidity being associated with more tolerant strains (45, 57), although another study suggests that less-fluid membranes are associated with more tolerant strains (58). In this study, we provide further support for the concept that low PE content is beneficial for ethanol tolerance. This result can guide engineering to improve ethanol tolerance toward the reduction of PE synthesis. This compound is produced by four separate pathways, but the Psd pathway, which utilizes PS as a substrate is predominant in *S. cerevisiae* (63, 64), so future works can be addressed in this direction.

In summary, the lipid compositions of most of the yeast strains in this study were comparable, but there were significant differences between these and the MY29 strain. Upon ethanol treatment, this composition changed significantly, and a more similar composition was reached, suggesting an adaptation mechanism in common with the other strains. Changes in saturation were observed for each of the strains upon ethanol treatment, but it is not clear whether these changes have a direct impact upon fluidity and tolerance, and it is likely that other factors beyond the scope of this study play a

critical role and further investigation is needed. The PE abundance of the least tolerant strain, MY26, was significantly higher than in the other strains. Our investigation therefore suggests that the membranes of more tolerant strains are more fluid and contain less PE. Overall, our results point to a reduced set of desirable membrane compositions and features that promote ethanol tolerance with increased fluidity and permeability appearing to be key.

MATERIALS AND METHODS

Strains and medium conditions. The *S. cerevisiae* yeast strains used in this study are listed in Table 2. A total of 61 strains from different isolation sources were selected. These strains were maintained in GPY-agar medium (%wt/vol: yeast extract, 0.5; peptone, 0.5; glucose, 2; agar, 2). Yeast identity was confirmed by sequencing the D1/D2 domain of the 26S rRNA gene (65).

Drop test experiments: assay in ethanol plates. To assess yeast strains' ethanol tolerance, drop test experiments were carried out. Rectangular GPY plates supplemented with different ethanol percentages (0, 6, 10, 14, 16, and 18%) were prepared. Yeast cells were grown overnight at 28°C on GPY media and diluted to an OD_{600} of 0.1 in sterile water. Then, serial dilutions of cells (10^{-1} to 10^{-3}) were transferred onto plates with replicates, followed by incubation at 28°C for 10 days with the plates wrapped in Parafilm to avoid ethanol evaporation. Each strain was inoculated twice on the same plate but at different positions, and an exact replicate of the plate was made. Using this method, four biological replicates of each strain were performed. Growth values were assigned to each of the replicates: 0, no growth; 1, weak growth; 2, intermediate growth; and 3, marked growth. Median growth values were assigned for each ethanol concentration. Hierarchical clustering used in heatmap plot was elaborated by using Heatmapper tool (66), with Euclidean distance measurement, and group clustering was based on growth in different ethanol medium averages (average linkage).

Assay in liquid media. (i) OD measurements. GPY precultures of each strain were prepared and incubated at 28°C overnight. These cultures were washed with sterile water and adjusted to an OD_{600} of 0.1 in each of the culture media (YNB liquid medium supplemented with different ethanol percentages [0, 1, 6, 8, 10, 13, 16, and 18%]). YNB is composed of 6.7 g/liter of amino acids and ammonium sulfate (YNB; Difco) and supplemented with 20 g/liter of D-glucose as a carbon source. Growth was monitored in a SPECTROstar Omega instrument (BMG Labtech, Offenburg, Germany) at 28°C. Nunc MicroWell 96-well plates (Thermo Fisher Scientific) wrapped in Parafilm and with water in each of its four repositories were used. Measurements were taken at 600 nm every 30 min, with 10 s of preshaking before each measurement until 64 h of growth monitoring. All the experiments were carried out in triplicate.

(ii) Estimation of the NIC and MIC parameters. The basis of the technique, used as described previously (40), is the comparison of the area under the OD–time curve of positive control (absence of ethanol, optimal conditions) with the areas of the tested condition (presence of ethanol, increasing inhibitory conditions). As the amount of inhibitor in the well increases, the effect on the growth of the organism also increases. This effect on the growth is manifested by a reduction in the area under the OD–time curve relative to the positive control at any specified time.

Briefly, the area under the OD–time curves were calculated by integration using GCAT software (http://gcat-pub.glbrc.org/). Then, for each ethanol condition and strain replicate, the fractional area (fa) was obtained by dividing the tested area between the positive-control area: fa = (test area)/(positive-control area). The plot of the fa versus $\log_{10}$ ethanol concentration produced a sigmoid-shape curve that could be well fitted with the modified Gompertz function for decay (67): $fa = A + C \times \exp[-\exp(B(x - M))]$, where A is the lowest asymptote of fa, B is the slope parameter, C is the distance between the upper and lower asymptotes, and M is the $\log_{10}$ ethanol concentration of the inflexion point. After this modeling, the NIC and MIC parameters could be estimated as described previously (66).

$$\mathrm{NIC} = 10^{[M-(1.718/B)]}$$

$$\mathrm{MIC} = 10^{[M+(1/B)]}$$

To check for significant differences among yeast species for NIC and MIC parameters, an analysis of variance was performed using the one-way ANOVA module of Statistica 7.0 software. Tukey's test was employed for mean comparison. The ggplot2 package (68) implemented in R software, version 3.2.2 (R Development Core Team, 2011), was used for graphic representations of the NIC and MIC values.

Strain selection and competition fermentation. Competition fermentations were carried out in 30 ml of GPY, GPY+6% ethanol, or GPY+10% ethanol in triplicate. 0.1 OD of each of the five strains (AJ4, MY3, MY14, MY26, and MY29) was inoculated in every initial culture. Every 3 or 5 days, 1 ml of the culture was transferred into the corresponding fresh medium. After 5 and 10 rounds, culture plates of samples from every tube were obtained. Then, 20 colonies from every plate were randomly picked for identification. This was carried out by means of mitochondrial digestion profile identification (69), which allowed differentiation of all the strains except for MY14 and MY29, which shared the same exact profile. As an alternative, since we had the genome sequences of MY14 and MY29 (70), we identified a divergent region among these two strains that comprises gene *MMS1*. We amplified a region of gene *MMS1* with the primers f1 (AACGGATCCTTTTTCCCAAC) and r1 (CGGTCGCAAAAATTAACG) and used RsaI digestion to

TABLE 2 List of the 61 *Saccharomyces* strains selected used in this study

Strain	Strain repository or collection	Isolation source and/or origin	Strain properties and/or description
Wine commercial fermentation strains			
MY1	Lallemand	Wine	White and rosé wines
MY2	Lallemand	Wine	White wines
MY3	Lallemand	Wine	Rosé and red wines
MY4	Lallemand	Wine	White and rosé wines
MY6	Lallemand	Wine	White, rosé, and red wines
MY7	Lallemand	Wine	Red wines
MY8	Lallemand	Wine	Red wines
MY11	Lallemand	Wine	White wines
MY12	Lallemand	Wine	Red wines
MY13	Lallemand	Wine	White, rosé, and red wines
MY14	Lallemand	Wine	Sparkling wines, fruit wines, and ciders
MY15	Lallemand	Wine	White wines
MY16	Lallemand	Wine	White, rosé, and red wines
MY17	Lallemand	Wine	White wines
MY18	Lallemand	Wine	Stuck fermentations
MY19	Lallemand	Wine	Red wines
MY20	Lallemand	Wine	Red wines
MY21	Lallemand	Wine	Red wines
MY51	Lallemand/AQ29[a]	Wine	Red wines
MY62	Lallemand	Wine	Red wines[b]
MY63	Lallemand	Wine	White and rosé wines
Wine noncommercial fermentation strains			
MY52	AQ1336	Wine, South Africa	
MY53	AQ923	Wine, Spain	
MY54	AQ924	Wine, Spain	
MY55	AQ2371	Bili wine, West Africa	
MY56	AQ2375	Bili wine, West Africa	
MY61	I.CF14[c]	Wine, Hungary	High temp
MY28	AQ2492	Flor wine, Spain	
MY29	AQ2356	Flor wine, Spain	
MY30	AQ94	Flor wine, Spain	
MY31	AQ636	Flor wine, Spain	
Other commercial fermentation strains			
AJ4	Lallemand	Fermentations	
MY50	Lallemand	Fermenting cacao	
MY60	Fermentis	Bioethanol	Ethanol red
Other noncommercial fermentation strains			
MY25	AQ2579	*Agave salmiana*, Peru	
MY26	AQ2493	*Agave salmiana*, Mexico	
MY27	AQ2591	Chicha de jora, Peru	
MY32	AQ594	Sake, Japan	
MY33	AQ1312	Sake, Japan	
MY34	AQ1314	Sake, Japan	
MY35	AQ2332	Chicha de jora, Peru	
MY36	AQ2469	Chicha de jora, Peru	
MY37	AQ2363	Masato, Peru	
MY38	AQ2473	Masato, Peru	
MY43	AQ1180	Cider, Ireland	
MY44	AQ1182	Cider, Ireland	
MY45	AQ1184	Cider, Ireland	
MY46	AQ2851	Sugar cane, Brazil	
MY47	AQ2543	Sugar cane, Brazil	
MY48	AQ2506	Sugar cane, Brazil	
MY57	AQ843	Beer, Belgium	

(Continued on next page)

TABLE 2 (Continued)

Strain	Strain repository or collection	Isolation source and/or origin	Strain properties and/or description
MY58	AQ1323	Sorghum beer, Burkina Faso	
MY49	AQ1085	Fermenting cacao, Indonesia	
MY59	UFLA	Bioethanol	
Natural environmental strains			
MY22	AQ2458	*Agelaia vicina*, Peru	
MY23	AQ2163	*Quercus faginea*, Spain	
MY24	AQ997	*Prunus armeniaca*, Hungary	
Clinical strains			
MY39	AQ2587	Dietetic product, Spain	
MY40	AQ2654	Feces, Spain	
MY41	AQ435	Vagina, Spain	
MY42	AQ2717	Lung, Spain	

[a]AQ, Amparo Querol collection.
[b]MY62 is an *S. cerevisiae* strain containing a limited amount of *S. kudriavzevii* genome (72, 73).
[c]Kindly provided by M. Sipiczki.

differentiate specially these two strains. Theoretical results for digestion bands sizes in an agarose gel were calculated based on Sanger sequencing of the amplicon for the strains of interest (see Fig. S3).

Lipid composition and membrane studies. (i) Lipid extraction and quantification by ammonium ferrothiocyanate assay. Yeast precultures of each one of the five selected strains (AJ4, MY3, MY12, MY26, and MY29) were first propagated in 25 ml of GPY medium at 200 rpm and 28°C. The cultures were harvested after 24 h, and total lipids were extracted by using a modified Bligh and Dyer protocol (71). To quantify the lipids, 10 μl of sample was taken from the above 100 μl of reconstituted lipids in chloroform and added to 2 ml of chloroform with 1 ml of assay reagent (0.1 M $FeCl_3 \cdot 6H_2O$, 0.4 M ammonium thiocyanate) in a 15-ml glass tube. Samples were vortexed for 1 min and centrifuged at 14,500 $\times$ *g* for 5 min. The lower layer was collected into quartz cuvettes. The absorbance was measured at 488 nm, and the concentration of lipid was determined by comparison with a standard curve of a mixture of phospholipid standards (POPC, POPE, and POPG; Sigma).

(ii) Mass spectrometry of lipids present in the strains. The lipids from each of the five yeast strains extracted as previously described were reconstituted in 100 μl of chloroform to contain 5 μg/μl lipid, as determined by ammonium ferrothiocyanate assay, and then diluted 1 in 50 in solvent A (50:50 acetonitrile-H_2O, 5 mM ammonium formate, and 0.1% [vol/vol] formic acid). Analysis of 10-μl samples was performed by liquid chromatography-mass spectrometry (LC-MS). LC was performed on a U3000 UPLC system (Thermo Scientific, Hemel Hempstead, United Kingdom) using a Kinetex C_{18} reversed-phase column (Phenomenex, 2.6 μm particle size, 2.1 mm $\times$ 150 mm) at a flow rate of 200 μl/min with a gradient from 10% solvent B to 100% solvent B (85:10:5 isopropanol-acetonitrile-H_2O, 5 mM ammonium formate, and 0.1% [vol/vol] formic acid) with the following profile: $t = 0$, 10% A; $t = 20$, 86%A; $t = 22$, 96%A; and $t = 26$, 95%A. MS analysis was carried out in positive- and negative-ionization modes on a Sciex 5600 Triple TOF. Source parameters were optimized on infused standards. Survey scans were collected in the mass range of 250 to 1,250 Da for 250 ms. MS/MS data were collected using top five information-dependent acquisition and dynamic exclusion for 5 s, using a fixed collision energy of 35 V and a collision energy spread of 10 V for 200 ms per scan. ProgenesisQI was used for quantification, and LipidBlast (https://fiehnlab.ucdavis.edu/projects/LipidBlast) was used for identification. All data were manually verified and curated. Data were analyzed by two-way ANOVA and the Tukey's multiple-comparison test, where $n = 5$. Data sets were uploaded to https://doi.org/10.17036/researchdata.aston.ac.uk.00000495.

TLC analysis. Yeast lipids extracted as described above after 24 h of growth were analyzed by TLC. Briefly, 20 μg of lipid sample and 10-μg portions of phospholipid lipid standards (POPE and POPS; Sigma) were loaded onto silica gel TLC plates (Sigma) and separated using chloroform-methanol-acetic acid-water (25:15:4:2). The plates were air dried, sprayed with ninhydrin reagent (0.2% ninhydrin in ethanol; Sigma), and charred at 100°C for 5 min. Images of the plates were captured with a digital camera, and the spot intensity was determined using ImageJ software.

Laurdan membrane fluidity assay. Yeast cultures were set up in GPY, followed by incubation at 200 rpm and 28°C overnight. Then, 25 ml of GPY medium containing 0, 6, or 10% ethanol was inoculated to an OD_{595} of 0.5. Samples were taken at different time points during the fermentation, and live yeast samples were diluted to an OD_{595} of 0.4 in GPY medium, followed by incubation with 5 μM Laurdan (6-dodecanoyl-2-dimethylaminonaphthalene) for 1 h. The fluorescence emission of these cells stained with Laurdan was determined using a microplate reader (Mithras; Berthold) with the following filters; $\lambda_{ex} = 460$ and $\lambda_{em} = 535$. Generalized polarization (GP), derived from fluorescence intensities at critical wavelengths, can be considered an index of membrane fluidity and is calculated as $GP = (I_{460} - I_{535})/(I_{460} + I_{535})$. Data were analyzed by one-way ANOVA and Tukey's multiple-comparison test, where $n = 3$.

Carboxyfluorescein dye leakage assay. Lipids for each of the five selected yeast strains extracted as described previously were used to generate 400-nm liposomes loaded with 100 mM CF in protein buffer (50 mM Tris, 50 mM NaCl [pH 7.4]). Dye leakage assays were performed with 0.125 mg/ml liposomes and increasing concentrations of ethanol in protein buffer at room temperature, and the fluorescence emission was measured (λ_{ex} = 492 nm, λ_{em} = 512 nm). Liposomes were treated with 5% Triton X-100 to fully disrupt them, and fluorescence measurements were normalized to the maximum reading for each liposome composition. Data were analyzed by one-way ANOVA and Tukey's multiple-comparison test, where $n = 3$.

PCA. To visualize the relationships among different ethanol tolerance parameters and lipid composition of the selected *S. cerevisiae* strains, a PCA was performed using the prcomp function and ggbiplot (0.55 version) and ggplot (3.2.1 version) implemented in R.

Data availability. The sequencing of the D1/D2 26S rRNA gene of the strains was deposited in GenBank with the accession numbers MW559910 to MW559970 (73).

SUPPLEMENTAL MATERIAL

Supplemental material is available online only.

SUPPLEMENTAL FILE 1, PDF file, 2 MB.

ACKNOWLEDGMENTS

M.L.-P. was supported by an FPU contract from Ministerio de Ciencia, Innovación y Universidades (FPU15/01775). This study was supported by projects ERA CoBioTech H2020 MeMBrane (grant agreement: 722361) to A.Q. and A.D.G., PCI2018-093190 (AEI/FEDER, UE) to A.Q., and BBSRC (BB/R02152X/1) to A.D.G.

REFERENCES

1. Smith MG, Snyder M. 2006. Yeast as a model for human disease. Curr Protoc Hum Genet Chapter 15:Unit 15.6. https://doi.org/10.1002/0471142905.hg1506s48.
2. Legras JL, Merdinoglu D, Cornuet JM, Karst F. 2007. Bread, beer and wine: *Saccharomyces cerevisiae* diversity reflects human history. Mol Ecol 16:2091–2102. https://doi.org/10.1111/j.1365-294X.2007.03266.x.
3. Arias García JA. 2008. Diversidad genética en las especies del complejo *Saccharomyces sensu stricto* de fermentaciones tradicionales. PhD thesis. Departament de Genètica, Universitat de València, Valencia, Spain.
4. Badotti F, Vilaça ST, Arias A, Rosa CA, Barrio E. 2014. Two interbreeding populations of *Saccharomyces cerevisiae* strains coexist in cachaça fermentations from Brazil. FEMS Yeast Res 14:289–301. https://doi.org/10.1111/1567-1364.12108.
5. Kodama K. 1993. Sake-brewing yeasts, p 129–168. *In* Rose AH, Harrison JS (ed), The yeasts, 2nd ed. Academic Press, London, United Kingdom.
6. Stringini M, Comitini F, Taccari M, Ciani M. 2009. Yeast diversity during tapping and fermentation of palm wine from Cameroon. Food Microbiol 26:415–420. https://doi.org/10.1016/j.fm.2009.02.006.
7. Suárez Valles B, Pando Bedriñana R, Fernández Tascón N, González Garcia A, Rodríguez Madrera R. 2005. Analytical differentiation of cider inoculated with yeast (*Saccharomyces cerevisiae*) isolated from Asturian (Spain) apple juice. LWT - Food Sci Technol 38:455–461. https://doi.org/10.1016/j.lwt.2004.07.008.
8. van Zyl WH, Lynd LR, den Haan R, McBride JE. 2007. Consolidated bioprocessing for bioethanol production using *Saccharomyces cerevisiae*, p 205–235. *In* Olsson L (ed), Biofuels. Springer Berlin Heidelberg, Berlin, Germany.
9. Eberlein C, Leducq JB, Landry CR. 2015. The genomics of wild yeast populations sheds light on the domestication of man's best (micro) friend. Mol Ecol 24:5309–5311. https://doi.org/10.1111/mec.13380.
10. Liti G, Carter DM, Moses AM, Warringer J, Parts L, James SA, Davey RP, Roberts IN, Burt A, Koufopanou V, Tsai IJ, Bergman CM, Bensasson D, O'Kelly MJT, van Oudenaarden A, Barton DBH, Bailes E, Nguyen AN, Jones M, Quail MA, Goodhead I, Sims S, Smith F, Blomberg A, Durbin R, Louis EJ. 2009. Population genomics of domestic and wild yeasts. Nature 458:337–341. https://doi.org/10.1038/nature07743.
11. Alba-Lois L, Segal-Kischinevzky C. 2010. Beer and wine makers. Nat Educ 3:17.
12. Camarasa C, Sanchez I, Brial P, Bigey F, Dequin S. 2011. Phenotypic landscape of *Saccharomyces cerevisiae* during wine fermentation: evidence for origin-dependent metabolic traits. PLoS One 6:e25147. https://doi.org/10.1371/journal.pone.0025147.
13. Franco-Duarte R, Mendes I, Umek L, Drumonde-Neves J, Zupan B, Schuller D. 2014. Computational models reveal genotype–phenotype associations in *Saccharomyces cerevisiae*. Yeast 31:265–277. https://doi.org/10.1002/yea.3016.
14. Suárez Valles B, Pando Bedriñana R, Fernández Tascón N, Querol Simón A, Rodríguez Madrera R. 2007. Yeast species associated with the spontaneous fermentation of cider. Food Microbiol 24:25–31. https://doi.org/10.1016/j.fm.2006.04.001.
15. Querol A, Fernández-Espinar MT, Del Olmo M, Barrio E. 2003. Adaptive evolution of wine yeast. Int J Food Microbiol 86:3–10. https://doi.org/10.1016/s0168-1605(03)00244-7.
16. Querol A, Barrio E, Ramón D. 1994. Population dynamics of natural *Saccharomyces* strains during wine fermentation. Int J Food Microbiol 21:315–323. https://doi.org/10.1016/0168-1605(94)90061-2.
17. Schuller D, Cardoso F, Sousa S, Gomes P, Gomes AC, Santos MAS, Casal M. 2012. Genetic diversity and population structure of *Saccharomyces cerevisiae* strains isolated from different grape varieties and winemaking regions. PLoS One 7:e32507. https://doi.org/10.1371/journal.pone.0032507.
18. Pando Bedriñana R, Querol Simón A, Suárez Valles B. 2010. Genetic and phenotypic diversity of autochthonous cider yeasts in a cellar from Asturias. Food Microbiol 27:503–508. https://doi.org/10.1016/j.fm.2009.11.018.
19. Ganucci D, Guerrini S, Mangani S, Vincenzini M, Granchi L. 2018. Quantifying the effects of ethanol and temperature on the fitness advantage of predominant *Saccharomyces cerevisiae* strains occurring in spontaneous wine fermentations. Front Microbiol 9:1563. https://doi.org/10.3389/fmicb.2018.01563.
20. Salvadó Z, Arroyo-López FN, Guillamón JM, Salazar G, Querol A, Barrio E. 2011. Temperature adaptation markedly determines evolution within the genus *Saccharomyces*. Appl Environ Microbiol 77:2292–2302. https://doi.org/10.1128/AEM.01861-10.
21. Salvadó Z, Arroyo-López FN, Barrio E, Querol A, Guillamón JM. 2011. Quantifying the individual effects of ethanol and temperature on the fitness advantage of *Saccharomyces cerevisiae*. Food Microbiol 28:1155–1161. https://doi.org/10.1016/j.fm.2011.03.008.
22. Jones RP, Greenfield PF, Wang L, Cai Y, Zhao X, Jia X, Zhang J, Liu J, Zhen H, Wang T, Tang XLY, J W. 1987. Ethanol and the fluidity of the yeast plasma membrane. Yeast 3:223–232. https://doi.org/10.1002/yea.320030403.
23. Lloyd D, Morrell S, Carlsen HN, Degn H, James PE, Rowlands CC. 1993. Effects of growth with ethanol on fermentation and membrane fluidity of *Saccharomyces cerevisiae*. Yeast 9:825–833. https://doi.org/10.1002/yea.320090803.

24. Marza E, Camougrand N, Manon S. 2002. Bax expression protects yeast plasma membrane against ethanol-induced permeabilization. FEBS Lett 521:47–52. https://doi.org/10.1016/s0014-5793(02)02819-3.
25. Alexandre H, Ansanay-Galeote V, Dequin S, Blondin B. 2001. Global gene expression during short-term ethanol stress in *Saccharomyces cerevisiae*. FEBS Lett 498:98–103. https://doi.org/10.1016/s0014-5793(01)02503-0.
26. Yang K-M, Lee N-R, Woo J-M, Choi W, Zimmermann M, Blank LM, Park J-B. 2012. Ethanol reduces mitochondrial membrane integrity and thereby impacts carbon metabolism of *Saccharomyces cerevisiae*. FEMS Yeast Res 12:675–684. https://doi.org/10.1111/j.1567-1364.2012.00818.x.
27. Zinser E, Sperka-Gottlieb CDM, Fasch EV, Kohlwein SD, Paltauf F, Daum G. 1991. Phospholipid synthesis and lipid composition of subcellular membranes in the unicellular eukaryote *Saccharomyces cerevisiae*. J Bacteriol 173:2026–2034. https://doi.org/10.1128/jb.173.6.2026-2034.1991.
28. Peña C, Arango R. 2009. Evaluación de la producción de etanol utilizando cepas recombinantes de *Saccharomyces cerevisiae* a partir de melaza de caña de azúcar. Dyna 159:153–161.
29. Ingram LO, Buttke TM. 1985. Effects of alcohols on micro-organisms. Adv Microb Physiol 25:253–300. https://doi.org/10.1016/s0065-2911(08)60294-5.
30. Sánchez-Gallego JI. 2009. Efecto de la quercetina y la rutina frente al daño oxidativo inducido en eritrocitos con distintos contenidos de colesterol. PhD thesis. Departamento de Bioquímica y Biología Molecular, Universidad de Salamanca, Salamanca, Spain.
31. Simonin H, Beney L, Gervais P. 2008. Controlling the membrane fluidity of yeasts during coupled thermal and osmotic treatments. Biotechnol Bioeng 100:325–333. https://doi.org/10.1002/bit.21749.
32. Chiou J-S, Krishna PR, Kamaya H, Ueda I. 1992. Alcohols dehydrate lipid membranes: an infrared study on hydrogen bonding. Biochim Biophys Acta Biomembr 1110:225–233. https://doi.org/10.1016/0005-2736(92)90363-Q.
33. Kranenburg M, Vlaar M, Smit B. 2004. Simulating induced interdigitation in membranes. Biophys J 87:1596–1605. https://doi.org/10.1529/biophysj.104.045005.
34. Vanegas JM, Faller R, Longo ML. 2010. Influence of ethanol on lipid/sterol membranes: phase diagram construction from AFM imaging. Langmuir 26:10415–10418. https://doi.org/10.1021/la1012268.
35. Lee AG. 2004. How lipids affect the activities of integral membrane proteins. Biochim Biophys Acta 1666:62–87. https://doi.org/10.1016/j.bbamem.2004.05.012.
36. Montecucco C, Smith GA, Dabbeni-Sala F, Johannsson A, Galante YM, Bisson R. 1982. Bilayer thickness and enzymatic activity in the mitochondrial cytochrome *c* oxidase and ATPase complex. FEBS Lett 144:145–148. https://doi.org/10.1016/0014-5793(82)80588-7.
37. Yuan C, O'Connell RJ, Feinberg-Zadek PL, Johnston LJ, Treistman SN. 2004. Bilayer thickness modulates the conductance of the BK channel in model membranes. Biophys J 86:3620–3633. https://doi.org/10.1529/biophysj.103.029678.
38. Leão C, Van Uden N. 1984. Effects of ethanol and other alkanols on passive proton influx in the yeast *Saccharomyces cerevisiae*. Biochim Biophys Acta 774:43–48. https://doi.org/10.1016/0005-2736(84)90272-4.
39. Tierney KJ, Block DE, Longo ML. 2005. Elasticity and phase behavior of DPPC membrane modulated by cholesterol, ergosterol, and ethanol. Biophys J 89:2481–2493. https://doi.org/10.1529/biophysj.104.057943.
40. Arroyo-López FN, Salvadó Z, Tronchoni J, Guillamón JM, Barrio E, Querol A. 2010. Susceptibility and resistance to ethanol in *Saccharomyces* strains isolated from wild and fermentative environments. Yeast 27:1005–1015. https://doi.org/10.1002/yea.1809.
41. Lairón-Peris M, Pérez-Través L, Muñiz-Calvo S, Guillamón JM, Heras JM, Barrio E, Querol A. 2020. Differential contribution of the parental genomes to a *S. cerevisiae* × *S. uvarum* hybrid, inferred by phenomic, genomic, and transcriptomic analyses, at different industrial stress conditions. Front Bioeng Biotechnol 8:129. https://doi.org/10.3389/fbioe.2020.00129.
42. Rossouw D, Bagheri B, Setati ME, Bauer FF. 2015. Co-flocculation of yeast species, a new mechanism to govern population dynamics in microbial ecosystems. PLoS One 10:e0136249. https://doi.org/10.1371/journal.pone.0136249.
43. Alonso-del-Real J, Lairón-Peris M, Barrio E, Querol A. 2017. Effect of temperature on the prevalence of *Saccharomyces cerevisiae* species against a *S. cerevisiae* wine strain in wine fermentation: competition, physiological fitness, and influence in final wine composition. Front Microbiol 8:150. https://doi.org/10.3389/fmicb.2017.00150.
44. Beaven MJ, Charpentier C, Rose AH. 1982. Production and tolerance of ethanol in relation to phospholipid fatty-acyl composition in *Saccharomyces cerevisiae* NCYC 431. J Gen Microbiol 128:1447–1455. https://doi.org/10.1099/00221287-128-7-1447.
45. Alexandre H, Rousseaux I, Charpentier C. 1994. Relationship between ethanol tolerance, lipid composition and plasma membrane fluidity in *Saccharomyces cerevisiae* and *Kloeckera apiculata*. FEMS Microbiol Lett 124:17–22. https://doi.org/10.1111/j.1574-6968.1994.tb07255.x.
46. Chi Z, Arneborg N. 1999. Relationship between lipid composition, frequency of ethanol-induced respiratory deficient mutants, and ethanol tolerance in *Saccharomyces cerevisiae*. J Appl Microbiol 86:1047–1052. https://doi.org/10.1046/j.1365-2672.1999.00793.x.
47. Learmonth RP, Gratton E. 2002. Assessment of membrane fluidity in individual yeast cells by laurdan generalized polarization and multi-photon scanning fluorescence microscopy, p 241–252. *In* Fluorescence spectroscopy. Springer, New York, NY.
48. Martínez P, Pérez Rodríguez L, Benítez T. 1997. Velum formation by flor yeasts isolated from sherry wine. Am J Enol Vitic 48:55–62.
49. Naumov GI. 2017. Genetic polymorphism of sherry *Saccharomyces cerevisiae* yeasts. Microbiol Russian Fed 86:19–31. https://doi.org/10.1134/S0026261716060151.
50. Aguilera F, Peinado RA, Millán C, Ortega JM, Mauricio JC. 2006. Relationship between ethanol tolerance, H^+-ATPase activity and the lipid composition of the plasma membrane in different wine yeast strains. Int J Food Microbiol 110:34–42. https://doi.org/10.1016/j.ijfoodmicro.2006.02.002.
51. Shobayashi M, Mitsueda SI, Ago M, Fujii T, Iwashita K, Iefuji H. 2005. Effects of culture conditions on ergosterol biosynthesis by *Saccharomyces cerevisiae*. Biosci Biotechnol Biochem 69:2381–2388. https://doi.org/10.1271/bbb.69.2381.
52. Navarro-Tapia E, Querol A, Pérez-Torrado R. 2018. Membrane fluidification by ethanol stress activates unfolded protein response in yeasts. Microb Biotechnol 11:465–475. https://doi.org/10.1111/1751-7915.13032.
53. Yoshikawa K, Tanaka T, Furusawa C, Nagahisa K, Hirasawa T, Shimizu H. 2009. Comprehensive phenotypic analysis for identification of genes affecting growth under ethanol stress in *Saccharomyces cerevisiae*. FEMS Yeast Res 9:32–44. https://doi.org/10.1111/j.1567-1364.2008.00456.x.
54. Bandara A, Fraser S, Chambers PJ, Stanley GA. 2009. Trehalose promotes the survival of *Saccharomyces cerevisiae* during lethal ethanol stress, but does not influence growth under sublethal ethanol stress. FEMS Yeast Res 9:1208–1216. https://doi.org/10.1111/j.1567-1364.2009.00569.x.
55. You KM, Rosenfield C-L, Knipple DC. 2003. Ethanol tolerance in the yeast *Saccharomyces cerevisiae* is dependent on cellular oleic acid content. Appl Environ Microbiol 69:1499–1503. https://doi.org/10.1128/aem.69.3.1499-1503.2003.
56. Henderson CM, Block DE. 2014. Examining the role of membrane lipid composition in determining the ethanol tolerance of *Saccharomyces cerevisiae*. Appl Environ Microbiol 80:2966–2972. https://doi.org/10.1128/AEM.04151-13.
57. Huffer S, Clark ME, Ning JC, Blanch HW, Clark DS. 2011. Role of alcohols in growth, lipid composition, and membrane fluidity of yeasts, bacteria, and archaea. Appl Environ Microbiol 77:6400–6408. https://doi.org/10.1128/AEM.00694-11.
58. Ishmayana S, Kennedy UJ, Learmonth RP. 2017. Further investigation of relationships between membrane fluidity and ethanol tolerance in *Saccharomyces cerevisiae*. World J Microbiol Biotechnol 33:1–10. https://doi.org/10.1007/s11274-017-2380-9.
59. Murzyn K, Róg T, Pasenkiewicz-Gierula M. 2005. Phosphatidylethanolamine-phosphatidylglycerol bilayer as a model of the inner bacterial membrane. Biophys J 88:1091–1103. https://doi.org/10.1529/biophysj.104.048835.
60. Dawaliby R, Trubbia C, Delporte C, Noyon C, Ruysschaert JM, Van Antwerpen P, Govaerts C. 2016. Phosphatidylethanolamine is a key regulator of membrane fluidity in eukaryotic cells. J Biol Chem 291:3658–3667. https://doi.org/10.1074/jbc.M115.706523.
61. Ballweg S, Sezgin E, Doktorova M, Covino R, Reinhard J, Wunnicke D, Hänelt I, Levental I, Hummer G, Ernst R. 2020. Regulation of lipid saturation without sensing membrane fluidity. Nat Commun 11:756. https://doi.org/10.1038/s41467-020-14528-1.
62. Jurešić GC, Blagović B, Rupčić J. 2009. Alterations in phosphatidylcholine and phosphatidylethanolamine content during fermentative metabolism in *Saccharomyces cerevisiae* brewer's yeast. Food Technol Biotechnol 47:246–252.

63. Birner R, Bürgermeister M, Schneiter R, Daum G. 2001. Roles of phosphatidylethanolamine and of its several biosynthetic pathways in *Saccharomyces cerevisiae*. Mol Biol Cell 12:997–1007. https://doi.org/10.1091/mbc.12.4.997.
64. Bürgermeister M, Birner-Grünberger R, Nebauer R, Daum G. 2004. Contribution of different pathways to the supply of phosphatidylethanolamine and phosphatidylcholine to mitochondrial membranes of the yeast *Saccharomyces cerevisiae*. Biochim Biophys Acta 1686:161–168. https://doi.org/10.1016/j.bbalip.2004.09.007.
65. Kurtzman CP, Robnett CJ. 1998. Identification and phylogeny of ascomycetous yeasts from analysis of nuclear large subunit (26S) ribosomal DNA partial sequences. Antonie Van Leeuwenhoek 98:331–371.
66. Babicki S, Arndt D, Marcu A, Liang Y, Grant JR, Maciejewski A, Wishart DS. 2016. Heatmapper: web-enabled heat mapping for all. Nucleic Acids Res 44:W147–W153. https://doi.org/10.1093/nar/gkw419.
67. Lambert RJW, Pearson J. 2000. Susceptibility testing: accurate and reproducible minimum inhibitory concentration (MIC) and non-inhibitory concentration (NIC) values. J Appl Microbiol 88:784–790. https://doi.org/10.1046/j.1365-2672.2000.01017.x.
68. Wickham H. 2009. ggplot2: elegant graphics for data analysis. Springer-Verlag, New York, NY.
69. Querol A, Barrio E, Ramón D. 1992. A comparative study of different methods of yeast strain characterization. Syst Appl Microbiol 15:439–446. https://doi.org/10.1016/S0723-2020(11)80219-5.
70. Morard M, Macías LG, Adam AC, Lairón-Peris M, Pérez-Torrado R, Toft C, Barrio E. 2019. Aneuploidy and ethanol tolerance in *Saccharomyces cerevisiae*. Front Genet 10:82. https://doi.org/10.3389/fgene.2019.00082.
71. Spickett CM, Reis A, Pitt AR. 2011. Identification of oxidized phospholipids by electrospray ionization mass spectrometry and LC-MS using a QQLIT instrument. Free Radic Biol Med 51:2133–2149. https://doi.org/10.1016/j.freeradbiomed.2011.09.003.
72. Erny C, Raoult P, Alais A, Butterlin G, Delobel P, Matei-Radoi F, Casaregola S, Legras JL. 2012. Ecological success of a group of *Saccharomyces cerevisiae*/*Saccharomyces kudriavzevii* hybrids in the Northern European wine-making environment. Appl Environ Microbiol 78:3256–3265. https://doi.org/10.1128/AEM.06752-11.
73. Lairon-Peris M, Querol A. 2021. Data from "Composition of membrane lipids reveals mechanisms of ethanol tolerance in the model yeast *Saccharomyces cerevisiae*". GenBank https://www.ncbi.nlm.nih.gov/nuccore/?term=MW559910:MW559970[accn]. *(Accession numbers.)*